Inorganic Chemistry
Article

Inorg. Chem. **2009**, *48*, 11551–11558 **11551**
DOI: 10.1021/ic901154m

Preparation, Facile Deprotonation, and Rapid H/D Exchange of the μ-Hydride Diiron Model Complexes of the [FeFe]-Hydrogenase Containing a Pendant Amine in a Chelating Diphosphine Ligand

Ning Wang,[†] Mei Wang,*[,†] Jihong Liu,[†] Kun Jin,[†] Lin Chen,[†] and Licheng Sun*[,†,‡]

[†]*State Key Laboratory of Fine Chemicals, DUT-KTH Joint Education and Research Center on Molecular Devices, Dalian University of Technology (DUT), Dalian 116012, China, and* [‡]*Department of Chemistry, Royal Institute of Technology (KTH), 10044, Stockholm, Sweden*

Received June 16, 2009

The CO-displacement of [(μ-pdt)$Fe_2(CO)_6$] with $(Ph_2PCH_2)_2N(n\text{-Pr})$ in refluxing toluene gave an unsymmetrical chelating complex [(μ-pdt){$Fe(CO)_3$}{$Fe(CO)(\kappa^2\text{-}Ph_2PCH_2N(n\text{-Pr})CH_2PPh_2$}] (**1**) as a major product, together with a small amount of the symmetrical intramolecular bridging complex [(μ-pdt){$\mu\text{-}Ph_2PCH_2N(n\text{-Pr})CH_2PPh_2$}{$Fe(CO)_2$}$_2$] (**2**) and the intermolecular bridging complex [{$\mu,\kappa^1,\kappa^1\text{-}Ph_2PCH_2N(n\text{-Pr})CH_2PPh_2$}{($\mu$-pdt)$Fe_2(CO)_5$}$_2$] (**3**). In contrast, the reaction of [(μ-pdt)$Fe_2(CO)_6$] with $(Ph_2PCH_2)_2NR$ (R = *n*-Pr, Ph) afforded the intermolecular bridging isomers **3** and **4** in the presence of a CO-removing reagent $Me_3NO\cdot 2H_2O$ in CH_3CN at room temperature. The molecular structures of **1**, **3**, and **4**, as well as the doubly protonated complex [**1**(H_NH_μ)]($OTf)_2$] were determined by X-ray analyses. The protonation processes of **1** with $HBF_4\cdot Et_2O$ and HOTf were studied in different solvents. The presence of the $H_\mu\cdots H_N$ interaction in [**1**(H_NH_μ)]$^{2+}$ was studied by relaxation time T_1 and spin saturation transfer measurements. The μ-hydride of [**1**(H_μ)]$^+$ and [**1**(H_NH_μ)]$^{2+}$ undergo facile deprotonation with aniline and rapid H/D exchange with deuterons in solution. In contrast, neither deprotonation nor H/D exchange was detected for [(μ-H)-(μ-pdt){$Fe(CO)_3$}{$Fe(CO)(\kappa^2$-dppp)}]$^+$ ([**5**(H_μ)]$^+$, dppp = $Ph_2PCH_2CH_2CH_2PPh_2$) without internal base.

Introduction

X-ray crystal structures show that the active site of [FeFe]-hydrogenases ([FeFe]-H_2ases) is composed of a [4Fe4S] cluster linked through a cysteine residue to the [2Fe2S] subcluster, in which the two iron atoms are bridged by a dithiolate cofactor.[1,2] Some spectroscopic and theoretical studies suggest that the dithiolate bridge is an azadithiolate (adt, $(SCH_2)_2NH$) or an oxadithiolate (odt, $(SCH_2)_2O$).[3,4] One interesting issue is the function of this internal base, either the bridging-N or -O atom, in the [FeFe]-H_2ase active site. On the basis of density functional theory (DFT) calculations and in the light of numerous examples for heterolytic H_2 activation mediated by transition metal complexes containing a pendant basic site,[5−9] it is proposed that the internal base near the iron centers could act as a proton transfer relay to provide a low energy pathway for H−H bond heterolytic cleavage and formation at the [FeFe]-H_2ase active site. Therefore, the preparation and the related chemistry of diiron dithiolate complexes containing internal bases have drawn intense attention for better understanding the mechanism of enzymatic hydrogen evolution. In recent years, protophilicity of the bridging-N atom of diiron azadithiolate complexes has been well-studied.[10−13] Very recently, Rauchfuss and co-workers reported the great influence of the bridging X (X = NH, O, CH_2) group of the dithiolate bridge on the protonation and deprotonation of the diiron model complexes.[14] Lubitz and co-workers have reported some strong experimental evidence from advanced electron paramagnetic resonance (EPR) studies, showing that the

*To whom correspondence should be addressed. E-mail: symbueno@dlut.edu.cn (M.W.); lichengs@kth.se (L.S.).

(1) Peters, J. W.; Lanzilotta, W. N.; Lemon, B. J.; Seefeldt, L. C. *Science* **1998**, *282*, 1853–1858.
(2) Nicolet, Y.; Piras, C.; Legrand, P.; Hatchikian, C. E.; Fontecilla-Camps, J. C. *Structure* **1999**, *7*, 13–23.
(3) Nicolet, Y.; Lacey, A. L.; Vernede, X.; Fernandez, V. M.; Hatchikian, E. C.; Fontecilla-Camps, J. C. *J. Am. Chem. Soc.* **2001**, *123*, 1596–1602.
(4) Pandey, A. S.; Harris, T. V.; Giles, L. J.; Peters, J. W.; Szilagyi, R. K. *J. Am. Chem. Soc.* **2008**, *130*, 4533–4540.
(5) Fan, H.-J.; Hall, M. B. *J. Am. Chem. Soc.* **2001**, *123*, 3828–3829.
(6) Custelcean, R.; Jackson, J. E. *Chem. Rev.* **2001**, *101*, 1963–1980.
(7) Rakowski DuBois, M.; DuBois, D. L. *Chem. Soc. Rev.* **2009**, *38*, 62–72.
(8) Ishiwata, K.; Kuwata, S.; Ikariya, T. *J. Am. Chem. Soc.* **2009**, *131*, 5001–5009.
(9) Yang, J. Y.; Morris Bullock, R.; Shaw, W. J.; Twamley, B.; Rakowski DuBois, M.; DuBois, D. L. *J. Am. Chem. Soc.* **2009**, *131*, 5935–5945.
(10) Lawrence, J. D.; Li, H.; Rauchfuss, T. B.; Bénard, M.; Rohmer, M.-M. *Angew. Chem., Int. Ed.* **2001**, *40*, 1768–1771.
(11) Barton, B. E.; Rauchfuss, T. B. *Inorg. Chem.* **2008**, *47*, 2261–2263.
(12) Schwartz, L.; Eilers, G.; Eriksson, L.; Gogoll, A.; Lomoth, R.; Ott, S. *Chem. Commun.* **2006**, 520–522.
(13) Wang, F.; Wang, M.; Liu, X.; Jin, K.; Dong, W.; Sun, L. *Dalton Trans.* **2007**, 3812–3919.
(14) Barton, B. E.; Olsen, M. T.; Rauchfuss, T. B. *J. Am. Chem. Soc.* **2008**, *130*, 16834–16835.

Published on Web 11/24/2009

central atom of the bridging ligand in the active site of FeFe-hydrogenases is indeed a nitrogen atom.[15]

In addition to the [FeFe] complexes with bridging azadithiolate ligands, DuBois and co-workers has demonstrated that the tertiary amine in the chelating diphosphine ligand $(R_2PCH_2)_2NR'$ (PNP) of mononuclear iron and nickel complexes significantly accelerates both H_2 uptake and production.[16−18] Similarly, a recent report by Talarmin and co-workers describes the protonation processes of [(μ-pdt)-{Fe(CO)$_3$}{Fe(CO)(κ^2-$Ph_2PCH_2N(Me)CH_2PPh_2$)}] (pdt = propane-1,3-dithiolate) with $HBF_4\cdot Et_2O$ in acetone and CH_2Cl_2, respectively, indicating that the great effect of solvents can even switch the N-protonated product to the μ-hydride. These reports show that the pendant amine of such a chelating diphosphine ligand can play a similar role as the N atom in the active site of the [FeFe] hydrogenase enzyme.[19]

Our studies described in this paper provide more important evidence for the function of the pendant amine in the diphosphine ligand of the diiron complex as relays for proton transfer to and from the iron centers. Here we report the CO-displacement of [(μ-pdt)Fe$_2$(CO)$_6$] with $(Ph_2PCH_2)_2N(R)$ (PNP, R = *n*-Pr, Ph) under different conditions for selective preparation of the unsymmetrical chelating complex [(μ-pdt){Fe(CO)$_3$}{Fe(CO)(κ^2-$Ph_2PCH_2N(n\text{-}Pr)CH_2PPh_2$)}] (**1**) and the intermolecular bridging complex [(μ,κ^1,κ^1-$Ph_2PCH_2N(R)CH_2PPh_2$){(μ-pdt)Fe$_2$(CO)$_5$}$_2$] (**3**, R = *n*-Pr; **4**, Ph). The protonation processes of **1** with $HBF_4\cdot Et_2O$ and HOTf as the proton source, the facile deprotonation of the μ-hydride of [**1**(H$_\mu$)]$^+$ and [**1**(H$_N$H$_\mu$)]$^{2+}$ in the presence of weak bases, the rapid H/D exchange of the μ-hydride of [**1**(H$_\mu$)]$^+$ and [**1**(H$_N$H$_\mu$)]$^{2+}$ with deuterons in solution, and the crystal structures of **1**, [**1**(H$_N$H$_\mu$)](OTf)$_2$,[20] **3**, and **4** are described in this paper. These systems are compared to an analogue system without internal base. The activity of the μ-hydride of [**1**(H$_\mu$)]$^+$ and [**1**(H$_N$H$_\mu$)]$^{2+}$ containing a pendant amine in the chelating diphosphine ligand contrasts with the relative inertness of the μ-hydride in the analogous complex [(μ-H)(μ-pdt){Fe(CO)$_3$}{Fe(CO)(κ^2-dppp)}] [**5**(H$_\mu$)]$^+$ and other previously reported diiron dithiolate complexes toward organic bases.[13,14,21,22]

Results and Discussion

CO−Displacement of [(μ-pdt)Fe$_2$(CO)$_6$] by PNP Ligands and Spectroscopic Characterization of Complexes 1−4. The products of three coordination modes were afforded by the CO-displacement of [(μ-pdt)Fe$_2$(CO)$_6$] with $(Ph_2PCH_2)_2N(n\text{-}Pr)$ in refluxing toluene for 3 h (Scheme 1). The unsymmetrical chelating complex [(μ-pdt){Fe(CO)$_3$}{Fe(CO)(κ^2-$Ph_2PCH_2N(n\text{-}Pr)CH_2PPh_2$)}]

Scheme 1

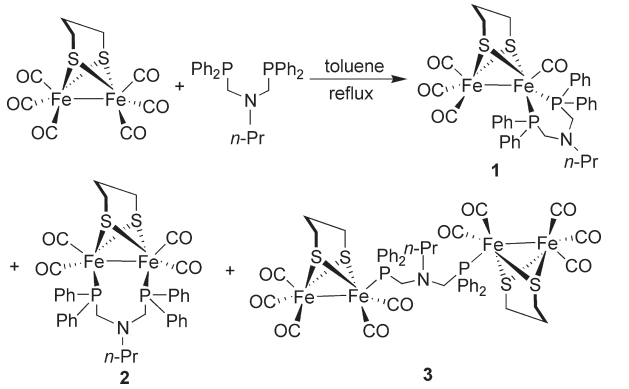

(**1**) was obtained as a major product, together with ca. 3% of the symmetrical intramolecular bridging complex [(μ-pdt)(μ-$Ph_2PCH_2N(n\text{-}Pr)CH_2PPh_2$){Fe(CO)$_2$}$_2$] (**2**) and 15% of the intermolecular bridging complex [{(μ-pdt)Fe$_2$(CO)$_5$}$_2$(μ,κ^1,κ^1-$Ph_2PCH_2N(n\text{-}Pr)CH_2PPh_2$)] (**3**). In the presence of a CO-removing reagent $Me_3NO\cdot 2H_2O$, the reaction of [(μ-pdt)Fe$_2$(CO)$_6$] and $(Ph_2PCH_2)_2N(n\text{-}Pr)$ in CH_3CN at room temperature for 3 h gave complex **3** in ca. 65% yield.[22] Therefore, the unsymmetrical chelating complex **1** and the intermolecular bridging complex **3** can be selectively prepared from the CO-displacement of [(μ-pdt)Fe$_2$(CO)$_6$] by controlling the reaction condition. When ligand $(Ph_2PCH_2)_2N(Ph)$ was used for the CO-displacement of [(μ-pdt)Fe$_2$(CO)$_6$], the intermolecular bridging complex [{(μ-pdt)Fe$_2$(CO)$_5$}$_2$(μ,κ^1,κ^1-$Ph_2PCH_2N(Ph)CH_2PPh_2$)] (**4**) was the sole product either in refluxing toluene or in the presence of $Me_3NO\cdot 2H_2O$ in CH_3CN at room temperature (Scheme 2), indicating that the group on the N atom has a great influence on the coordination style of the PNP ligand. Selective preparation of these coordination isomers and the chemistry of unsymmetric diphosphine diiron complexes are of particular interest as the unsymmetric [2Fe2S] complexes are attractive functional models of the [FeFe]-hydrogenase active site.

Complex **1** was doubly protonated in diethyl ether upon addition of 3 equiv of HOTf. The proton−hydride diiron complex [**1**(H$_N$H$_\mu$)](OTf)$_2$ was obtained as a purple crystalline solid in good yield after washing with diethyl ether and recrystallized in hexane/CH_2Cl_2. Complex **1** is stable in the solid state and in solution under an N_2 atmosphere, while its doubly protonated species [**1**(H$_N$H$_\mu$)](OTf)$_2$ is very sensitive to moisture.

Complexes **1**−**4** and [**1**(H$_N$H$_\mu$)](OTf)$_2$ were characterized by MS, IR, ^{1}H and ^{31}P NMR spectroscopy, and **1**, **3**, **4**, and [**1**(H$_N$H$_\mu$)](OTf)$_2$ were also identified by elemental analysis. The IR data of the ν(CO) bands of **1**−**4** are listed in Table 1 together with the ν(CO) data of the reference complex [(μ-pdt){Fe(CO)$_3$}{Fe(CO)(κ^2-dppp)}] (**5**; dppp = $Ph_2PCH_2CH_2CH_2PPh_2$).[22] The band at 1894 cm^{-1} for **1** is attributed to the vibration of the CO ligand in the Fe(CO)(κ^2-$Ph_2PCH_2N(n\text{-}Pr)CH_2PPh_2$) unit of **1**, while the bands at 1948 and 2020 cm^{-1} are assigned to the CO vibrations of the Fe(CO)$_3$ unit.[23] A comparison of the

(15) Silakov, A.; Wenk, B.; Reijerse, E.; Lubitz, W. *Phys. Chem. Chem. Phys.* **2009**, 6592–6599.
(16) Curtis, C. J.; Miedaner, A.; Ciancanelli, R. F.; Ellis, W. W.; Noll, B. C.; Rakowski DuBois, M.; DuBois, D. L. *Inorg. Chem.* **2003**, *42*, 216–227.
(17) Henry, R. M.; Shoemaker, R. K.; Newell, R. H.; Jacobsen, G. M.; DuBois, D. L.; Rakowski DuBois, M. *Organometallics* **2005**, *24*, 2481–2491.
(18) Henry, R. M.; Shoemaker, R. K.; DuBois, D. L.; DuBois, M. R. *J. Am. Chem. Soc.* **2006**, *128*, 3002–3010.
(19) Ezzaher, S.; Capon, J.-F.; Gloaguen, F.; Pétillon, F.; Schollhammer, P.; Talarmin, J. *Inorg. Chem.* **2009**, *48*, 2–4.
(20) Wang, N.; Wang, M.; Zhang, T.; Li, P.; Liu, J.; Sun, L. *Chem. Commun.* **2008**, 5800–5802.
(21) Gloaguen, F.; Lawrence, J. D.; Rauchfuss, T. B. *J. Am. Chem. Soc.* **2001**, *123*, 9476–9477.
(22) Adam, F. I.; Hogarth, G.; Kabir, S. E.; Richards, I. *C. R. Chim.* **2008**, *11*, 890–905.
(23) Wang, N.; Wang, M.; Liu, T.; Li, P.; Eriksson, L.; Zhang, T.; Darensbourg, M. Y.; Sun, L. *Inorg. Chem.* **2008**, *47*, 6948–6955.

Scheme 2

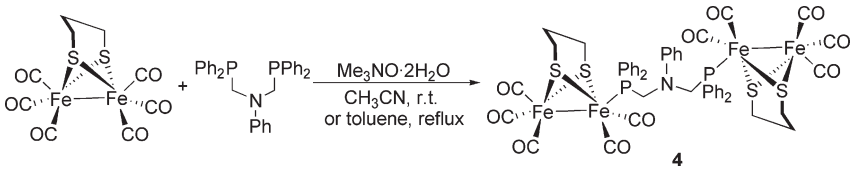

Table 1. Comparison of ν(CO) Bands of **1**–**5**

complex	ν(CO) (cm^{-1}) in CH_2Cl_2
1	2020, 1948, 1894
2	1981, 1943, 1909
3	2040, 1973, 1924
4	2041, 1975, 1924
5	2019, 1946, 1890

ν(CO) data of **1** and **2** shows that the frequency of the first ν(CO) band of **1** is apparently higher than that of the corresponding band displayed by the symmetrically disubstituted diiron complex **2**, whereas the frequency of the last ν(CO) band of **1** is lower than the corresponding ν(CO) frequency of **2**. Complexes **3** and **4** display similar ν(CO) data in the range of 1924−2041 cm^{-1}. A comparison of the ν(CO) absorptions of **1** and **5** shows that the electron density of their iron centers is similar.

Molecular Structures of 1, 3, 4, and [1(H$_N$H$_\mu$)](OTf)$_2$. The molecular structures of **1**, **3**, **4**, and [**1**(H$_N$H$_\mu$)](OTf)$_2$ are determined by X-ray diffraction studies of single crystals, which are shown in Figure 1 as ball and stick drawings. Selected bond lengths and angles for **1**, **3**, **4**, and [**1**(H$_N$H$_\mu$)](OTf)$_2$ are listed in Table 2.

The central [2Fe2S] structure of complex **1** has a butterfly framework, and each iron atom is coordinated with a pseudosquare-pyramidal geometry. The iron atoms of complex [**1**(H$_N$H$_\mu$)](OTf)$_2$ are coordinated with a distorted octahedral geometry as previously reported μ-hydride diiron dithiolate models.[12,13] In the solid state, the $(Ph_2PCH_2)_2N(n\text{-}Pr)$ ligand lies in the apical/basal configuration at the Fe(2) atom of **1**, while the orientation of the two phosphorus atoms in the crystal of [**1**(H$_N$H$_\mu$)](OTf)$_2$ changes to a basal/basal position. The different coordination modes lead to the single bond rotation of the Fe(2)PCNCP cyclohexane ring. The Fe(2) atom points down and the N atom is up in the chair conformation of **1**, while a rotated chair conformation is observed for [**1**(H$_N$H$_\mu$)]$^{2+}$ with the hydrogen attached to the N atom on the axial bond. The Fe(2)−C(4) bonds of 1.740(4) Å for **1** and 1.737(4) Å for [**1**(H$_N$H$_\mu$)]$^{2+}$ are notably shorter than the three Fe(1)−C bonds 1.781−1.810 Å. Accordingly, the C(4)−O(4) distance is longer than the C−O distances in the Fe(CO)$_3$ unit of **1** and [**1**(H$_N$H$_\mu$)]$^{2+}$. A reasonable explanation is that the higher electron density of the Fe(2) atom leads to the stronger electron back-donation to the C(4)O(4) as compared to the back-donation from the Fe(1) center to the CO ligands. After protonation at the iron atoms, the Fe−Fe distance is increased by 0.056 Å and the H$_N$···H$_\mu$ distance is 3.934 Å in the molecule of the doubly protonated species [**1**(H$_N$H$_\mu$)](OTf)$_2$.

The main framework of complexes **3** and **4** are very similar. Each end of the zigzag P−C−N−C−P bridge is linked with a [2Fe2S] butterfly unit by coordination of the phosphorus atom to the Fe center in a basal position.[24] The Fe−Fe distances are 2.5202(11) and 2.5129(7) Å in **3** and **4**, respectively.

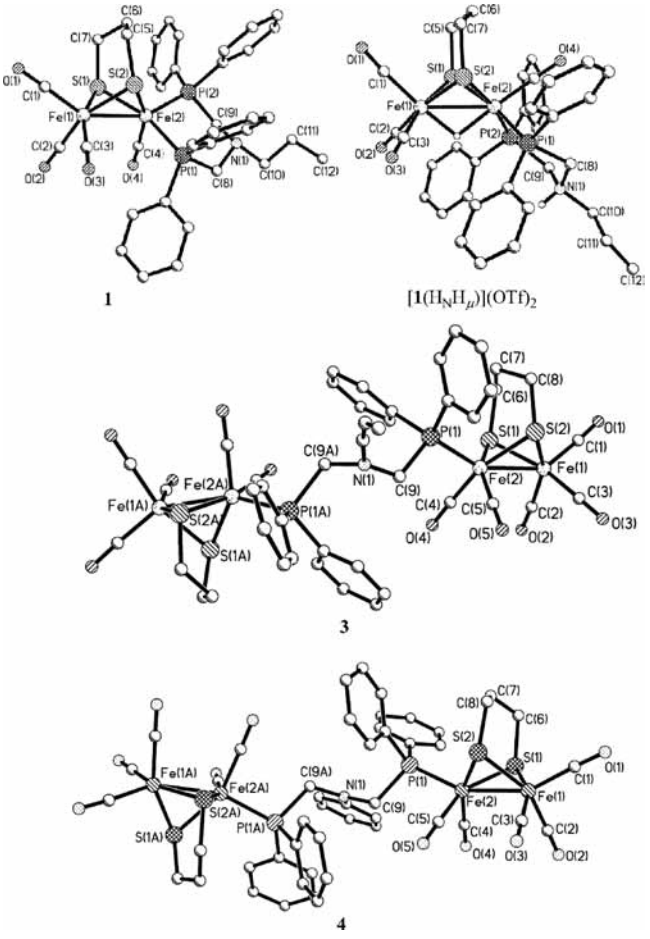

Figure 1. Molecular structures of **1**, **3**, **4**, and [**1**(H$_N$H$_\mu$)](OTf)$_2$ as ball and stick drawings.

Protonation and Deprotonation Processes of 1 and 5. To explore the influence of solvents and acids on the formation of [**1**(H$_\mu$)]$^+$ and [**1**(H$_N$)]$^+$, we first studied the protonation of **1** with HOTf in different solvents (d_6-acetone and CD_2Cl_2). As 1 equiv of HOTf was dropped into the d_6-acetone solution of **1**, three new signals at δ 37.3, 57.7, and 58.4 ppm appeared in the ^{31}P NMR spectrum (Figure 2b) in addition to the ^{31}P NMR signal of **1** at δ 52.5 ppm (Figure 2a).[20] The ^{31}P NMR signals at δ 57.7 and 58.4 ppm are attributed to the H$_N$-endo/exo isomers of [**1**(H$_N$)]$^+$, and the ^{31}P NMR signal at δ 37.3 ppm is assigned to the phosphorus atoms of the μ-hydride complex [**1**(H$_\mu$)]$^+$. Further addition of HOTf up to 3 equiv

(24) Gao, W.; Ekstrom, J.; Liu, J.; Chen, C.; Eriksson, L.; Weng, L.; Åkermark, B.; Sun, L. *Inorg. Chem.* **2007**, *46*, 1981–1991.

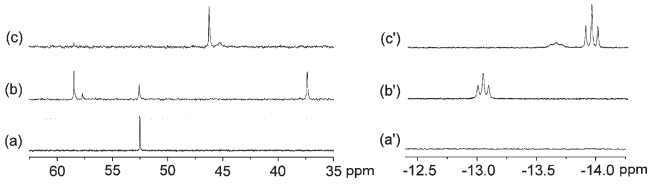

Figure 2. Selected regions of the $^{31}P\{^1H\}$ (left) and ^1H (right) NMR spectra of **1** in d_6-acetone with (a) +0 equiv, (b) +1 equiv HOTf, and (c) +2 equiv HOTf to that in part b at 298 K.

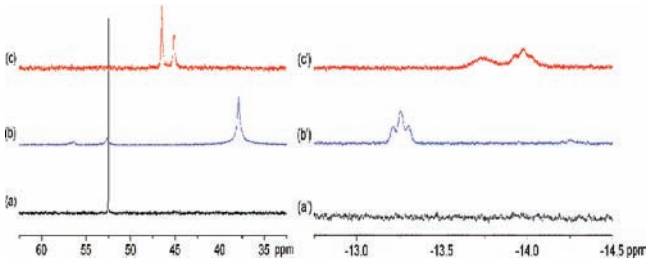

Figure 3. Selected regions of the $^{31}P\{^1H\}$ (left) and ^1H (right) NMR spectra of **1** in CD_2Cl_2 with (a) +0 equiv, (b) +1 equiv HOTf, and (c) +2 equiv HOTf to that in part b at 298 K.

Table 2. Selected Bond Lengths (Å) and Angles (deg) for **1**, **3**, **4**, and $[\mathbf{1}(H_NH_\mu)](OTf)_2$

	1	$[\mathbf{1}(H_NH_\mu)]^{2+}$	**3**	**4**
Fe(1)−Fe(2)	2.5564(7)	2.6121(16)	2.5202(11)	2.5129(7)
Fe(1)−S(1)	2.2594(10)	2.2497(16)	2.2518(17)	2.2603(10)
Fe(1)−S(2)	2.2643(11)	2.2527(16)	2.2472(16)	2.2554(11)
Fe(2)−S(1)	2.2525(10)	2.2595(16)	2.2647(18)	2.2685(10)
Fe(2)−S(2)	2.2592(10)	2.2500(16)	2.2547(16)	2.2628(10)
Fe−P(1)	2.2132(11)	2.2182(17)	2.2395(16)	2.2324(9)
Fe−P(2)	2.1981(10)	2.2313(15)		2.2244(9)
Fe(1)−C_{av}	1.785	1.806	1.791	1.788
Fe(2)−C_{av}	1.740(4)	1.737(4)	1.757	1.771
Fe−$H(100)_{av}$		1.659		
N(1)−H(101)		0.893(18)		
Fe−S−Fe	68.92	70.87	67.96	67.45
S−Fe−S	84.62	84.11	84.56	84.71
P−Fe(2)−P	92.51(4)	95.82(6)		
Fe−Fe−P(1)	109.54(3)	113.85(4)	153.02(6)	155.69
Fe−Fe−P(2)	154.00(4)	113.01(5)		

results in complete disappearance of the ^{31}P NMR signals at δ 37.3, 52.5, 57.7, and 58.4 ppm for $[\mathbf{1}(H_\mu)]^+$, **1**, and the endo/exo isomers of $[\mathbf{1}(H_N)]^+$, respectively, accompanied with the appearance of two new signals at δ 45.1 and 46.2 ppm ascribed to the doubly protonated species $[\mathbf{1}(H_NH_\mu)]^{2+}$ (Figure 2c).

For the protonation of **1** in the presence of 1 equiv of HOTf in CD_2Cl_2, the $[\mathbf{1}(H_\mu)]^+$ was formed as a dominant product contaminated with $[\mathbf{1}(H_N)]^+$ as assayed by ^1H and ^{31}P NMR spectroscopy (Figure 3b). Upon addition of HOTf up to 3 equiv, the H_N-endo/exo isomers of the doubly protonated species were formed (Figure 3c). The results show that the formation of $[\mathbf{1}(H_N)](OTf)$ is preferred in acetone over methylene chloride.

Then we studied the protonation of **1** with $HBF_4\cdot Et_2O$ in CD_2Cl_2. When 2 equiv of $HBF_4\cdot Et_2O$ was added to the CD_2Cl_2 solution of **1**, the only new signal at δ 38.0 ppm in the ^{31}P NMR spectrum (Figure 4b) and the signal at δ −13.0 ppm in the ^1H NMR spectrum show that the μ-hydride diiron complex $[\mathbf{1}(H_\mu)]^+$ is formed instantly and quantitatively,[11−14] and the N-protonated species $[\mathbf{1}(H_N)]^+$ is not detected. This is in agreement with the

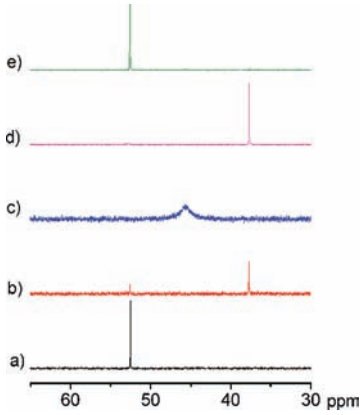

Figure 4. Selected region of the $^{31}P\{^1H\}$ NMR of **1** in CD_2Cl_2 with (a) +0 equiv, (b) +2 equiv $HBF_4\cdot Et_2O$, (c) +5 equiv $HBF_4\cdot Et_2O$ to that in part b, (d) +5 equiv aniline to that in part c, and (e) +2 equiv aniline to that in part d at 298 K.

report by Talarmin and co-workers.[19] The results indicate that, in addition to the solvent, the strength of the acid used also has a certain influence on the formation of the singly protonated species of **1**. Further addition of $HBF_4\cdot Et_2O$ up to 7 equiv results in immediate disappearance of the ^{31}P NMR signal for $[\mathbf{1}(H_\mu)]^+$ and simultaneous appearance of a broad ^{31}P NMR signal at δ 45.5 ppm (Figure 4c), which is ascribed to the doubly protonated complex $[\mathbf{1}(H_NH_\mu)]^{2+}$ (Scheme 3).

It is noticeable a broad ^{31}P NMR signal for the two isomers appears in Figure 4c when $HBF_4\cdot Et_2O$ is used at room temperature in CD_2Cl_2. In contrast, when HOTf is used as a proton source under the same condition, two sharp ^{31}P NMR signals for the endo and exo isomers of $[\mathbf{1}(H_NH_\mu)]^{2+}$ are observed (Figure 3c), indicating that the interconversion of the endo and exo isomers is slow. The result implies that the BF_4^- anion could assist intermolecular proton transfer.[18] The interconversion of the endo and exo isomers can be speeded up as temperature is increased. The two ^{31}P NMR signals gradually merge into a relatively broad signal (see Supporting Information Figure S1) with increase of the temperature from 25 to 70 °C in CD_3CN, which can only occur by intermolecular proton exchange.

To find the influence of the internal amine of the PNP ligand on the protonation of the diiron complexes, a comparative study of the reference complex [(μ-pdt){Fe(CO)$_3$}{Fe(CO)(κ^2-dppp)}] (**5**) without internal base in the chelating diphosphine ligand was made in parallel with complex **1**. With addition of 7 equiv of $HBF_4\cdot Et_2O$ to the CD_2Cl_2 solution of **5**, the signals for the μ-hydride species of **5** are not observed in the ^1H and ^{31}P NMR spectra. Complex **5** can be protonated by 1.5 equiv of HOTf or by a large excess of $HBF_4\cdot Et_2O$ to form the μ-hydride diiron complex $[\mathbf{5}(H_\mu)]^+$ (structure **C** of Figure 5).[22]

Formation of the μ-hydride on the Fe−Fe center makes the first and the last ν(CO) absorptions of **1** shift by 77 and 66 cm^{-1} to higher energy (Table 3), respectively. For the further protonation at the bridged N atom of the PNP ligand, the shift of 8 cm^{-1} for the first ν(CO) band of $[\mathbf{1}(H_\mu)]^+$ is identical to the shift reported for the protonation at the N atom of [(μ-pdt){Fe(CO)$_3$}{Fe(CO)-(κ^2-$Ph_2PCH_2N(Me)CH_2PPh_2$)}] (**6**).[19] As the similarity

Scheme 3

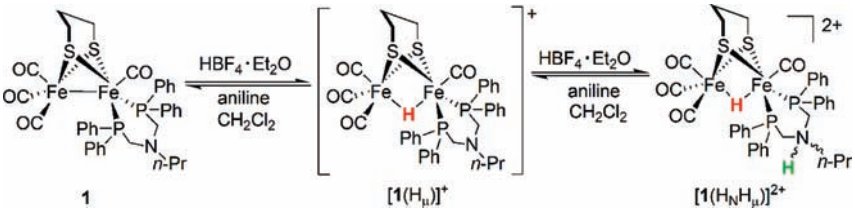

Table 3. Comparison of ν(CO) Bands of $[\mathbf{1}(H_\mu)]BF_4$, $[\mathbf{1}(H_NH_\mu)](OTf)_2$, and Analogous Protonated Diiron Complexes

complex	ν(CO) in CD_2Cl_2 (cm^{-1})	$\Delta\nu(CO)_{first}$ (cm^{-1})[a]	$\Delta\nu(CO)_{last}$ (cm^{-1})[b]
$[\mathbf{1}(H_\mu)]BF_4$	2097, 2037, 2003, 1960	77	66
$[\mathbf{1}(H_NH_\mu)](OTf)_2$	2105, 2057, 2043, 1990	85	96
$[\mathbf{5}(H_\mu)]OTf$	2095, 2040, 2003, 1956	77	66
$[\mathbf{6}(H_\mu)]BF_4$[c]	2099, 2052, 2036, 1961	79	68

[a] $\Delta\nu(CO)_{first} = \nu(CO)_{(first)protonated} - \nu(CO)_{(first)nonprotonated}$. [b] $\Delta\nu(CO)_{last} = \nu(CO)_{(last)protonated} - \nu(CO)_{(last)nonprotonated}$. [c] Reference 19.

of the ν(CO) bands for complexes **1** and **5**, the CO vibrations of $[\mathbf{1}(H_\mu)]^+$ are quite close to those of $[\mathbf{5}(H_\mu)]^+$.

As 5 equiv of aniline was added to the CD_2Cl_2 solution of $[\mathbf{1}(H_NH_\mu)]^{2+}$, the proton at the amine N atom was selectively deprotonated to regenerate $[\mathbf{1}(H_\mu)]^+$ quantitatively (Figure 4d). The μ-hydride $[\mathbf{1}(H_\mu)]^+$ was further deprotonated to the parent complex **1** when another 2 equiv of aniline was successively added (Figure 4e, Scheme 3). It is interesting to note that the μ-hydride of $[\mathbf{1}(H_\mu)]^+$ is so active that even a small amount of water results in the immediate deprotonation to form **1**. In a striking contrast, upon addition of 20 equiv of aniline to the CD_2Cl_2 solution of $[\mathbf{5}(H_\mu)]^+$, no deprotonated complex was detected during 5 h by the in situ IR and ^{31}P NMR.[21] In terms of the close similarity of the IR spectra in the ν(CO) region for $[\mathbf{1}(H_\mu)]^+$ and $[\mathbf{5}(H_\mu)]^+$ (Table 3), the electron density of their iron centers should be quite similar. The disparate activity of $[\mathbf{1}(H_\mu)]^+$ from $[\mathbf{5}(H_\mu)]^+$ is undoubtedly caused by the presence of an internal amine in the diphosphine ligand and more importantly by the short distance between the hydride and the internal base in $[\mathbf{1}(H_\mu)]^+$. It is reported that the terminal hydride in $[Fe_2(t\text{-}H)(\mu\text{-adt})(CO)_2(dppv)_2]^+$ (dppv = *cis*-1,2-bis(diphenylphosphino)ethylene) was immediately deprotonated with PBu_3 even at −90 °C, while its analogue $[Fe_2(t\text{-}H)(\mu\text{-pdt})(CO)_2(dppv)_2]$ without internal base could not be deprotonated.[14] If we compare the structure of $[\mathbf{1}(H_\mu)]^+$ (structure **B** of Figure 5) with that of the terminal hydride in a diiron azadithiolate complex (structure **A** of Figure 5), we can find a conformation of the (μ-H)FePCN unit in $[\mathbf{1}(H_\mu)]^+$ similar to the (*t*-H)FeSCN unit in the *t*-hydride diiron azadithiolate model complexes. By single bond rotation, the μ-hydride of $[\mathbf{1}(H_\mu)]^+$ can stand proximal to the amine N atom in the chelating diphosphine ligand, just like a *t*-hydride located near the amine N atom in the azadithiolate bridge. This could be a rational explanation for the similar deprotonation reactivity of the μ-hydride in $[\mathbf{1}(H_\mu)]^+$ with that of the *t*-hydride in the diiron azadithiolate complexes.

Studies on the $H_\mu\cdots H_N$ Interaction and the H/D Exchange. The presence of an $H_\mu\cdots H_N$ interaction in

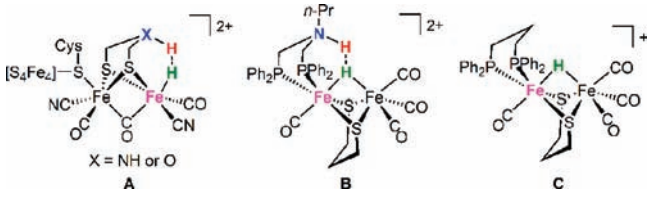

Figure 5. Structures of the proposed [2Fe2S] subcluster with a *t*-hydride (**A**, *t* = terminal), the μ-hydride diiron mimic $[\mathbf{1}(H_NH_\mu)]^{2+}$ (**B**), and the μ-hydride complex $[\mathbf{5}(H_\mu)]^+$ (**C**).

$[\mathbf{1}(H_NH_\mu)]^{2+}$ is supported by relaxation time T_1. The T_1 for the hydride signal of $[\mathbf{1}(H_\mu)]^+$ at δ −13.0 ppm was measured in CD_2Cl_2 at room temperature and was found to be 1243 ms. In comparison, the T_1 values for the two hydride signals at δ −13.6 and −13.9 ppm for the endo and exo isomers of $[\mathbf{1}(H_NH_\mu)]^{2+}$, respectively, were found to be 724 and 963 ms. The shorter relaxation time T_1 (724 ms) for the H_N-endo isomer than 1243 and 963 ms for $[\mathbf{1}(H_\mu)]^+$ and the H_N-exo isomer, respectively, suggests some degree of hydrogen-bonding interaction between the hydride (H_μ) and the proton (H_N) in $[\mathbf{1}(H_NH_\mu)]^{2+}$.[25] In addition, it was observed that irradiation of the hydride signal at δ −13.6 ppm led to an approximately 40% decrease in the intensity of the H_N-endo signal at δ 9.48 ppm in ^1H NMR at −70 °C in d_6-acetone, while irradiation of the hydride signal at δ −13.9 ppm under the same condition could not result in any decrease of the intensity of the H_N-exo signal at δ 10.45 ppm. The spin saturation transfer experiment gives another evidence for the $H_\mu\cdots H_N$ interaction in $[\mathbf{1}(H_NH_\mu)]^{2+}$.

The catalytic activity for H/D exchange is one of the important properties of hydrogenases.[26,27] The previous reported H/D exchange reactions via the μ-hydrides diiron model complexes without pendant bases require a preformed open site on the Fe center created by photolysis, and the rate of the H/D exchange is quite slow.[28−30] The deprotonation activity of the μ-hydride derived from **1** prompted us to study the H/D exchange of $[\mathbf{1}(H_\mu)]^+$ and $[\mathbf{1}(H_NH_\mu)]^{2+}$ with deuterons in solution. The protonated complexes $[\mathbf{1}(H_\mu)](BF_4)$ and $[\mathbf{1}(H_NH_\mu)](OTf)_2$ were prepared respectively by the reaction of **1** with $HBF_4\cdot Et_2O$ or HOTf. Since $[\mathbf{1}(H_\mu)]^+$ and $[\mathbf{1}(H_NH_\mu)]^{2+}$ are completely deprotonated in the presence of water, we chose a weak

(25) Chu, H. S.; Lau, C. P.; Wong, K. Y. *Organometallics* **1998**, *17*, 2768–2777.
(26) Albracht, S. P. J. *Biochim. Biophys. Acta* **1994**, *1188*, 167–204.
(27) Frey, M. *ChemBioChem* **2002**, *3*, 153–160.
(28) Zhao, X.; Georgakaki, I. P.; Miller, M. L.; Mejia-Rodriguez, R.; Chiang, C. Y.; Darensbourg, M. Y. *Inorg. Chem.* **2002**, *41*, 3917–3928.
(29) Zhao, X.; Georgakaki, I. P.; Miller, M. L.; Yarbrough, J. C.; Darensbourg, M. Y. *J. Am. Chem. Soc.* **2001**, *123*, 9710–9711.
(30) Georgakaki, I. P.; Miller, M. L.; Darensbourg, M. Y. *Inorg. Chem.* **2003**, *42*, 2489–2494.

Scheme 4

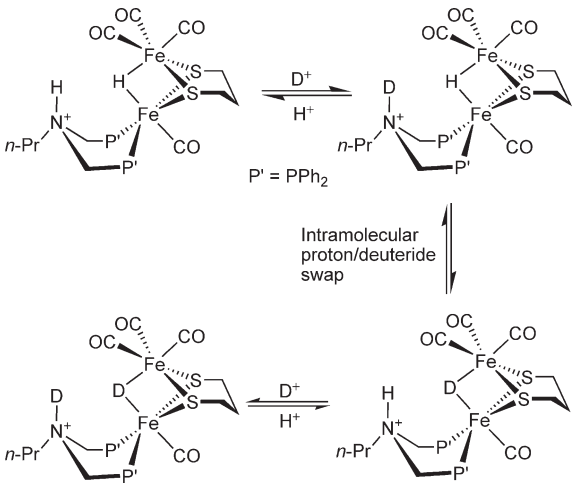

acid, CH_3COOD, as a deuteron source for H/D exchange reaction. The H/D exchange reactions of $[\mathbf{1}(H_\mu)](BF_4)$ and $[\mathbf{1}(H_NH_\mu)](OTf)_2$ with CH_3COOD in CH_2Cl_2 were monitored by ^1H and ^2H NMR spectroscopy at room temperature. Upon addition of 10 equiv of CH_3COOD to the CH_2Cl_2 solutions of $[\mathbf{1}(H_\mu)](BF_4)$ and $[\mathbf{1}(H_NH_\mu)](OTf)_2$, respectively, the signals at δ −13.0 ppm for the μ-hydride of $[\mathbf{1}(H_\mu)]^+$ and δ −13.6 and −13.9 ppm for $[\mathbf{1}(H_NH_\mu)]^{2+}$ disappeared instantly in the ^1H NMR spectra. In the meantime, a signal at high field appeared in each ^2H NMR spectrum, which are attributed to the μ-deuterides of $[\mathbf{1}(D_\mu)]^+$ and $[\mathbf{1}(D_ND_\mu)]^{2+}$. In addition, the broad signal at δ = 13.0 ppm is ascribed to the D-enriched CH_3COOD, which overlaps the signal of the deuteron on N atom in $[\mathbf{1}(D_ND_\mu)]^{2+}$. The spectroscopic evidence shows that the quick intermolecular H/D exchange does occur between the μ-hydride from $[\mathbf{1}(H_\mu)]^+$ or $[\mathbf{1}(H_NH_\mu)]^{2+}$ and the deuteron from CH_3COOD in solution.

To probe the role of the pendant amine of the diiron dithiolate models in the intermolecular H/D exchange, the control reaction was made with the in situ formed complex $[\mathbf{5}(H_\mu)](OTf)$, which was characterized by IR, ^1H, and $^{31}P\{^1H\}$ NMR spectroscopy (see the Experimental Section).[22] After addition of 10 equiv of CH_3COOD to the solution of $[\mathbf{5}(H_\mu)](OTf)$, the high-field signal at δ −12.8 ppm for $[\mathbf{5}(H_\mu)]^+$ did not show observable change during 5 h of monitoring by ^1H NMR, and except for the broad signal at δ 13.0 ppm for CH_3COOD, no other signal appeared in the ^2H NMR spectrum. The inertness of the μ-hydride in $[\mathbf{5}(H_\mu)]^+$ toward H/D exchange undoubtedly indicates the crucial role of the pendant amine proximal to the μ-hydride in the rapid intermolecular H/D exchange of the μ-hydride in $[\mathbf{1}(H_\mu)]^+$ and $[\mathbf{1}(H_NH_\mu)]^{2+}$ with deuterons in solution. To the best of our knowledge, the rapid H/D exchange has not been reported for the μ-hydride in the diiron dithiolate complexes.

Because H/D exchange was not observed for the protonated reference complex $[\mathbf{5}(H_\mu)]^+$ in the presence of CH_3COOD, the mechanism by direct exchange of the μ-hydride with deuterons in solution can be excluded. A proposed process for H/D exchange between $[\mathbf{1}(H_NH_\mu)]^{2+}$ and CH_3COOD is shown in Scheme 4. The observed exchange of the μ-hydride of $[\mathbf{1}(H_NH_\mu)]^{2+}$ with

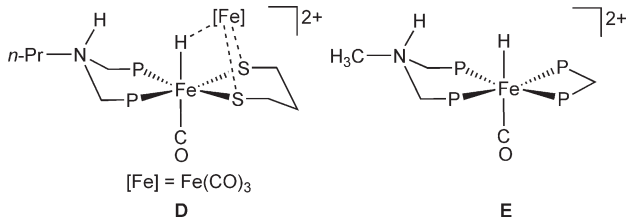

Figure 6. Comparison of the Structures of $[(\mu\text{-H})Fe(\mu\text{-pdt})(CO)\{Ph_2PCH_2N(n\text{-Pr})CH_2PPh_2\}]^{2+}$ unit (**D**) in $[\mathbf{1}(H_NH_\mu)]^{2+}$ and the DuBois' complex *trans*-$[HFe(dmpm)(CO)\{Et_2PCH_2N(CH_3)CH_2PEt_2\}]^{2+}$ (**E**).

deuterons in solution presumably involves a rapid intermolecular H/D exchange between the protonated built-in ammonium and CH_3COOD followed by a fast intramolecular proton/deuteride swap. As the N atom of the $Ph_2PCH_2N(n\text{-Pr})CH_2PPh_2$ ligand cannot be protonated by acetic acid in CH_2Cl_2, the observed H/D exchange of the μ-hydride of $[\mathbf{1}(H_\mu)]^+$ may involve an electrostatic interaction of the pendant amine and the deuteron of CH_3COOD in the initial stage. Several examples of intramolecular proton/hydride swap in pendant amine- or pyridine-containing complexes have been reported previously.[6,18] A dihydrogen intermediate is proposed for intramolecular proton/hydride exchange in *trans*-$[HFe(PNHP)(dmpm)(CO)]^{2+}$ (PNP = $Et_2PCH_2N(CH_3)CH_2PEt_2$, dmpm = $Me_2PCH_2PMe_2$).[18] The intermediate in our case is still not clear up to now. The dihydrogen intermediate is preferred in the light of the close similarity in the coordination structure of the $[(\mu\text{-H})Fe(\mu\text{-pdt})(CO)\{Ph_2PCH_2N(n\text{-Pr})CH_2PPh_2\}]^{2+}$ unit (structure **D** of Figure 6), if the $Fe(CO)_3$ moiety in $[\mathbf{1}(H_NH_\mu)]^{2+}$ is ignored, with that of the complex *trans*-$[HFe(dmpm)(CO)\{Et_2PCH_2N(CH_3)CH_2PEt_2\}]^{2+}$ (structure **E** of Figure 6).[18]

Conclusions

The unsymmetrical chelating complex **1** and the intermolecular bridging complex **3** can be selectively prepared from the CO-displacement of $[(\mu\text{-pdt})Fe_2(CO)_6]$ with $(Ph_2PCH_2)_2N(n\text{-Pr})$ by controlling the reaction condition. The doubly protonated diiron complex $[\mathbf{1}(H_NH_\mu)](OTf)_2$ was successfully isolated and crystallographically characterized, which shows the hydride H_μ^- and the proton H_N^+ in $[\mathbf{1}(H_NH_\mu)]^{2+}$ are close to each other (with a distance of 3.934 Å). The relaxation time T_1 and the results obtained from spin saturation transfer measurements support the presence of an $H_\mu\cdots H_N$ interaction in $[\mathbf{1}(H_NH_\mu)]^{2+}$. The facile deprotonation and rapid H/D exchange of the μ-hydride in the diiron complexes $[\mathbf{1}(H_\mu)]^+$ and $[\mathbf{1}(H_NH_\mu)]^{2+}$ with deuterons in solution provide an effective model of the active μ-hydride for the [FeFe]-H_2ase active site. The results obtained from comparative studies of analogous complexes $[\mathbf{1}(H_\mu)]^+$ and $[\mathbf{5}(H_\mu)]^+$ suggest that the built-in amine base in the flexible PNP ligand is capable of serving as an efficient proton transfer relay in the diiron μ-hydride complex. The built-in amine in the PNP ligand may approach the μ-hydride by the conformational change and make the μ-hydride in the diiron complex so active as to be deprotonated by weak bases and to occur via rapid H/D exchange with deuterons in solution, while the amine unit in the adt-bridge, being in the opposite position of the μ-hydride, can hardly influence the reactivity of the μ-hydride of the diiron dithiolate complex.[13,14,21,22] These results provide a new active model for the

proton transfer either to or from the iron center at the [2Fe2S] subcluster of the [FeFe]-H_2ase active site.

Experimental Section

Reagents and Instruments. All reactions and operations related to organometallic complexes were carried out under dry and oxygen-free dinitrogen with standard Schlenk techniques. Solvents were dried and distilled prior to use according to the standard methods. Commercially available chemicals, 1,3-propanedithiol, $Fe(CO)_5$, $PHPh_2$, *n*-propylamine, aniline, dppp, and $Me_3NO\cdot 2H_2O$ were reagent grade and used as received. Compounds $Ph_2PCH_2N(n\text{-}Pr)CH_2PPh_2$, $Ph_2PCH_2N(Ph)CH_2PPh_2$, [(μ-pdt)$Fe_2(CO)_6$], and [(μ-pdt){$Fe(CO)_3$}{$Fe(CO)(\kappa^2$-dppp)}] (**5**) were prepared according to literature methods.[22,31−33]

Infrared spectra were recorded on JASCO FT/IR 430 spectrometer. Proton and ^{31}P NMR spectra were collected with a Varian INOVA 400NMR instrument. Mass spectra were recorded on an HP1100 MSD mass spectrometer. Elemental analyses were performed with a Thermoquest-Flash EA 1112 elemental analyzer.

Synthesis of [(μ-pdt){$Fe(CO)_3$}{$Fe(CO)(\kappa^2$-$Ph_2PCH_2N(n$-$Pr)CH_2PPh_2$)}] (1), [(μ-pdt)(μ-$Ph_2PCH_2N(n$-$Pr)CH_2PPh_2$)$Fe_2(CO)_4$] (2), and [{$Fe_2(CO)_5(\mu$-pdt)}$_2(\mu,\kappa^1,\kappa^1$-$Ph_2PCH_2N(n$-$Pr)CH_2PPh_2$)] (3). Ligand $Ph_2PCH_2N(n\text{-}Pr)CH_2PPh_2$ (0.47 g, 1.0 mmol) was added to the toluene solution (20 mL) of [(μ-pdt)$Fe_2(CO)_6$] (0.39 g, 1.0 mmol). The red solution was refluxed for 3 h, and the color turned dark red. The solvent was removed under reduced pressure. The solid was extracted several times with hexane/CH_2Cl_2 (5:1, v/v). The residue was then purified by chromatography on a silica gel column with hexane/CH_2Cl_2 (3:1, v/v) as eluent. Complex **1** was obtained as a brown powder from the collected yellow band after removal of solvent. Yield: 0.61 g (78%). Single crystals suitable for X-ray analysis were obtained by recrystallization from hexane/CH_2Cl_2. ^{1}H NMR ($CDCl_3$): δ 7.71−7.20 (m, 20H, 4Ph), 3.76 (s, 2H, PCH_2N), 3.28 (s, 2H, PCH_2N), 2.44 (br s, 2H, NCH_2C), 1.68 (br s, 2H, $SCCH_2CS$), 1.45 (br s, 4H, SCH_2C), 1.30 (br s, 2H, $NCCH_2$), 0.87 (br s, 3H, CCH_3). ^{31}P NMR ($CDCl_3$): δ 52.5. IR (CH_2Cl_2): ν_{CO} = 2020, 1948, 1894 cm^{-1}. ESI-MS: *m*/*z* 786.1 (100%) [M + H]$^+$. Elem. anal. calcd for $C_{36}H_{37}Fe_2NO_4P_2S_2$: C, 55.05; H, 4.75; N, 1.78. Found: C, 55.05; H, 4.73; N, 1.85.

The extracts are combined and the solvent was removed under reduced pressure. The crude products were further separated by rechromatography on a silica gel column with hexane/CH_2Cl_2 (5:1, v/v) as eluent. Complexes **2** and **3** were respectively obtained.

Complex 2. Yield: 0.03 g (3%). ^{1}H NMR ($CDCl_3$): δ 7.75−7.40 (m, 20H, 4Ph), 3.57−3.42 (s, 4H, PCH_2N), 2.06−1.19 (m, 10H, $SCH_2CH_2CH_2S$, NCH_2CH_2), 0.87 (s, 3H, CCH_3). ^{31}P NMR ($CDCl_3$): δ 61.6. IR (CH_2Cl_2): ν_{CO} = 1981, 1943, 1909 cm^{-1}. ESI-MS: *m*/*z* 786.1 (100%) [M + H]$^+$. Elem. anal. calcd for $C_{36}H_{37}Fe_2NO_4P_2S_2$: C, 55.05; H, 4.75; N, 1.78. Found: C, 55.57; H, 4.83; N, 1.73.

Complex 3. Yield: 0.12 g (15%). Single crystals suitable for X-ray analysis were obtained by recrystallization from hexane/CH_2Cl_2. ^{1}H NMR ($CDCl_3$): δ 7.75−7.40 (m, 20H, 4Ph), 3.91 (s, 4H, PCH_2N), 2.19 (s, 2H, NCH_2C), 1.72−1.26 (m, 14H, $SCH_2CH_2CH_2S$, $NCCH_2$), 0.88 (s, 3H, CCH_3). ^{31}P NMR ($CDCl_3$): δ 56.3. IR (CH_2Cl_2): ν_{CO} = 2040, 1973, 1924 cm^{-1}. ESI-MS: *m*/*z* 1171.8 (100%) [M + H]$^+$, 1193.8 (45%) [M + Na]$^+$. Elem. anal. calcd for $C_{45}H_{43}Fe_4NO_{10}P_2S_4$: C, 46.14; H, 3.70; N, 1.20. Found: C, 45.97; H, 3.75; N, 1.23.

Synthesis of [{$Fe_2(CO)_5(\mu$-pdt)}$_2(\mu,\kappa^1,\kappa^1$-$Ph_2PCH_2N(Ph)$-CH_2PPh_2)] (4). CO-removing reagent $Me_3NO\cdot 2H_2O$ (0.29 g, 2.6 mmol) was added to the solution of **1** (1.0 g, 2.6 mmol) in CH_3CN (40 mL). The solution was stirred for 5 min, and then $Ph_2PCH_2N(Ph)CH_2PPh_2$ (0.636 g, 1.3 mmol) was added. After the mixture was reacted for 3 h at room temperature, a red powder was deposited from the solvent and washed several times with acetonitrile and hexane. Yield: 1.57 g (86%). Single crystals suitable for X-ray analysis were obtained by recrystallization from hexane/CH_2Cl_2. ^{1}H NMR ($CDCl_3$): δ 7.64−7.29 (m, 20H, 4Ph), 6.62−6.34 (m, 5H, Ph), 4.35 (s, 4H, PCH_2N), 1.67−1.25 (m, 12H, $SCH_2CH_2CH_2S$). ^{31}P NMR ($CDCl_3$): δ 60.3. IR (CH_2Cl_2): ν_{CO} = 2041, 1975, 1924 cm^{-1}. ESI-MS: *m*/*z* 1227.8 (100%) [M + Na]$^+$, 1205.8 (25%) [M + H]$^+$. Elem. anal. calcd for $C_{48}H_{41}Fe_4NO_{10}P_2S_4$: C, 47.83; H, 3.43; N, 1.16. Found: C, 47.68; H, 3.50; N, 1.21.

Synthesis of [(μ-H)(μ-pdt){$Fe(CO)_3$}{$Fe(CO)(\kappa^2$-Ph_2PCH_2-$N(n$-$Pr)CH_2PPh_2$)}](BF_4) [1(H_μ)](BF_4). A 2 equiv portion of $HBF_4\cdot Et_2O$ was added to the solution of **1** (0.79 g, 1.0 mmol) in CH_2Cl_2 (30 mL), and the red solution was stirred for 5 min. The solvent was removed under reduced pressure. The residue was washed several times with hexane/CH_2Cl_2 (10:1, v/v). Yield: 0.60 g (68%). ^{1}H NMR (CD_2Cl_2): δ 7.57−7.32 (m, 20H, 4Ph), 4.29 (m, 2H, PCH_2N), 3.25 (m, 2H, PCH_2N), 3.07 (br s, 2H, NCH_2C), 2.39−1.58 (m, 8H, $SCH_2CH_2CH_2S$, $NCCH_2$), 0.86 (br s, 3H, CCH_3), −13.0 (br s, μ-*H*). ^{31}P NMR (CD_2Cl_2): δ 37.3. IR (CH_2Cl_2): ν_{CO} = 2097, 2037, 2003, 1960 cm^{-1}.

Synthesis of [(μ-H)(μ-pdt){$Fe(CO)_3$}{$Fe(CO)(\kappa^2$-Ph_2PCH_2-$NH(n$-$Pr)CH_2PPh_2$)}](OTf)$_2$, [1(H_NH_μ)](OTf)$_2$. A 3 equiv portion of HOTf was added to a solution of **1** (0.79 g, 1.0 mmol) in diethyl ether (100 mL), and the yellow solution was stirred for 5 min. A purple powder was deposited from the solvent. It was washed several times with diethyl ether and dried in vacuum (yield: 0.95 g, 88%). Single crystals suitable for X-ray analysis was obtained by gentle addition of hexane to the CH_2Cl_2 solution of the freshly formed [1(H_NH_μ)](OTf)$_2$ (hexane/CH_2Cl_2 = 5:1, v/v). After the solution stood for one day at room temperature, some dark purple crystals of [1(H_NH_μ)](OTf)$_2$ appeared in the Schlenk tube. ^{1}H NMR (d_6-acetone): δ 10.1 (br, 1H, N*H*), 7.71−7.21 (m, 20H, 4Ph), 5.47−4.95 (m, 4H, PCH_2N), 3.97−3.76 (br s, 2H, NCH_2C), 3.28−1.88 (m, 8H, $SCH_2CH_2CH_2S$, $NCCH_2$), 0.98 (br s, 3H, CCH_3), −13.6 (t, μ-*H*, J_{H-P} = 19.9 Hz, H_N-endo isomer), −13.9 (t, μ-*H*, J_{H-P} = 20.1 Hz, H_N-exo isomer). ^{31}P NMR (d_6-acetone): δ 46.2, 45.1. IR (CH_2Cl_2): ν_{CO} = 2105, 2057, 2043, 1990 cm^{-1}. Elem. anal. calcd for $C_{38}H_{41}F_6Fe_2NO_{11}P_2S_4$: C, 41.36; H, 3.74; N, 1.27. Found: C, 41.30; H, 3.78; N, 1.24.

Synthesis of [(μ-H)(μ-pdt){$Fe(CO)_3$}{$Fe(CO)(\kappa^2$-dppp)}](OTf) (dppp = $Ph_2PCH_2CH_2CH_2PPh_2$), [5(H_μ)](OTf). Complex [**5**(H_μ)](OTf) was formed in situ by addition of 1.5 equiv of HOTf to the solution of **5** in CD_2Cl_2. The color of the solution immediately turned red. ^{1}H NMR (CD_2Cl_2): δ 7.75−7.10 (m, 20H, 4Ph), 2.80−1.65 (m, 12H, all CH_2), −12.8 (t, μ-*H*, J_{H-P} = 15.8 Hz). ^{31}P NMR (CD_2Cl_2): δ 43.5, 38.6. IR (CH_2Cl_2): ν_{CO} = 2095, 2040, 2003, 1956 cm^{-1}.

Measurements of Relaxation Time T_1 and Spin Saturation Transfer Experiments (400 MHz). Relaxation times (T_1) of the μ-hydride signals, at δ −13.0 for [1(H_μ)]$^+$, δ −13.6 for the H_N-endo isomer of [1(H_NH_μ)]$^{2+}$, and δ −13.9 for the H_N-exo isomer, were measured in CD_2Cl_2 solution at room temperature on a Bruker AVANCE II 400 instrument by the inversion−recovery method using the standard 180°−τ−90° pulse sequence and analyzing with the spectrometer T_1 routine. Spin saturation transfer experiments were carried out on the d_6-acetone solution of [1(H_NH_μ)]$^{2+}$. After the sample was cooled to −70 °C, the δ −13.6 resonance was irradiated for 10 s ($> 5T_1$) with irradiation power of 47 dB and the integrated intensity of the δ 9.48 resonance for the H_N-endo signal was recorded with the δ 4.95 signal (PCH_2N) as a reference. Subsequently, the δ −13.9

(31) Wu, W.; Li, C. *Chem. Commun.* **2003**, 1668–1669.
(32) Balch, A. L.; Olmstead, M. M.; Rowley, S. P. *Inorg. Chim. Acta* **1990**, *168*, 255–264.
(33) Lyon, E. J.; Georgakaki, I. P.; Reibenspies, J. H.; Darensbourg, M. Y. *Angew. Chem., Int. Ed.* **1999**, *38*, 3178–3180.

resonance was irradiated under the same experimental condition and the intensity of the δ 10.45 resonance for the H_N-exo signal was integrated. Diminution of the H_N-endo signal at δ 9.48 ppm was observed with irradiation of δ −13.6 ppm signal, while the integrated intensity of H_N-exo signal at δ 10.45 ppm did not show any detectable suppression with irradiation of δ −13.9 ppm signal.

Crystal Structure Determination of 1, 3, 4, and [1(H$_N$H$_\mu$)](OTf)$_2$. Crystallographic data of **1**, **3**, **4**, and [**1**(H_NH_μ)](OTf)$_2$ were collected on a Bruker Smart Apex II CCD diffractometer with graphite monochromated Mo Kα radiation (λ = 0.71073 Å) at 298 K using the $\omega-2\theta$ scan mode. Data processing was accomplished with the SAINT processing program. Intensity data were corrected for absorption by the SADABS program. The structures were solved by direct methods and refined on F^2 against full-matrix least-squares methods using the SHELX-97 program package.[34] All non-hydrogen atoms were refined anisotropically. Hydrogen atoms were placed by geometrical calculation and refined in a riding model. The μ-hydride and the proton on the N atom of [**1**(H_NH_μ)](OTf)$_2$ were located by the difference Fourier map.

(34) Sheldrick, G. M. *SHELXTL97*; University of Göttingen, Germany, 1997.

Acknowledgment. This work was supported by the National Natural Science Foundation of China (Grant no. 20633020), the National Basic Research Program of China (Grant No. 2009CB220009), the Program for Changjiang Scholars and Innovative Research Team in University (IRT0711), the Swedish Energy Agency, the Swedish Research Council, and the K & A Wallenberg Foundation of Sweden.

Supporting Information Available: X-ray crystallographic data of complexes **3** and **4** in CIF format. Selected region of variable-temperature ^{31}P NMR spectra of the endo and exo isomers of [**1**(H_NH_μ)](OTf)$_2$. This material is available free of charge via the Internet at http://pubs.acs.org.